

# Sedimentary Environment and Sequence Stratigraphy of the Lower Cretaceous Deposits in the Bideshk Area, at North of Esfahan, Iran

Mahboubeh Anari<sup>1\*</sup>, Nader Kohansal Ghadimvand<sup>1</sup>, Abdolhosein Kangazian<sup>2</sup> and Sayed Hasan Hejazi<sup>2</sup>

<sup>1</sup>Department of Geology, North Tehran Branch, Islamic Azad University, Tehran, Iran; M.Anari546@yahoo.com, nkohansal@yahoo.com

<sup>2</sup>Department of Geology, Khorasgan Branch, Islamic Azad University, Esfahan, Iran; kangazian@khuisf.ac.ir, hhejazi2010@yahoo.com

## Abstract

**Background/Objectives:** Rocks of the Mesozoic era in Iran, especially Cretaceous period, have been studied frequently from stratigraphic point of view, but little research has been done from sedimentology viewpoint. This study aims to restore the sedimentation condition and the conditions governing the sedimentary basins during that period (lower Cretaceous).

**Methods:** One stratigraphic section was measured along the outcrop in Bideshk Area, at North of Esfahan. 63 thin sections samples were studied to determine the facies and a polarized microscope was used for the procedure. **Findings:** Based on lithological properties, 3 lithostratigraphic units have identified in the area. Facies analysis and field observations led to identification of 10 carbonate facies, 4 terrigenous facies and also 4 mixed (terrigenous and carbonate). Bideshk area was deposited on a homoclinal ramp setting within four zones including Continental, tidal flat, lagoon and bar environments. Sequence stratigraphic analysis identified three third-order depositional sequences in the studied area. Lower boundary in the first sequence is unconformity first-type boundary (SB1) (with Jurassic deposits) and consists of Transgressive Systems Tract (TST). Sequence number 2 consists of Low stand Systems Tract (LST), Transgressive Systems Tract (TST) and High stand Systems Tract (HST). Sequence 3 also consists of LST, TST and HST. **Application:** These results could be used for comparison with other worldwide localities and provide additional data for lower Cretaceous paleogeographic reconstructions.

**Keywords:** Carbonate Facies, Sedimentary Environment, Sequence Stratigraphy

## 1. Introduction

In Early cretaceous there were some micro continental plate in central zone of Iran that a narrow and elongate oceanic (or near to oceanic) basin separated them. This empiric sea covered most part of the central zone of Iran and its sediments have experienced swift changes and different thicknesses in their facies. Wide stratigraphic gap and unconformity between lower cretaceous sediment and ancient rocks indicated that sediment environment of the central zone of Iran has been unstable. In most parts on this zone, an angular unconformity between lower

cretaceous orbitolina limestone and basement rocks points to Cimmerian. Probably these limestone rocks reach back to Barremian, Aptian and in some cases to Albian.<sup>1</sup>

Esfahan lower cretaceous records are quit complete. Therefore, investigation of their sedimentary environment and sequence stratigraphy is very important.

Considering that there is no any comprehensive and accurate sedimentology study on deposits in north of Esfahan (Bideshk), facies analyzing and reconstruction of sedimentary model of the basin in lower cretaceous in this area has been considered.

\*Author for correspondence

This study focuses on one of the lower cretaceous successions of the Esfahan area that is located near Bideshk village at north of Esfahan. The Lower Cretaceous succession in Bideshk area composed of sandstone, limestone, and mixed (terrigenous and limestone). The thickness of these sediments is 250m. This section is located in north of Esfahan and in the range of 33°23'19.1" N and 51°27'47.4" E on anti-klein of Bideshk (Figure 1).

This study tends to achieve the following goals:

- Identifying the sedimentary facies of Bideshk area in the studied thin sections.
- Determining facies column and curve of changes in depth, associated with the depositions of Bideshk area in the studied thin sections and field observation.
- Interpreting the sedimentary environment of the deposits of Bideshk area and presenting a sedimentary model consistent with the results of the studies.
- Recognizing the sedimentary sequences, sequence boundary and parasequence accumulation pattern, for drawing relative fluctuations curve of sea level in this area.

## 2. Methodology

One stratigraphic section was measured along the outcrop in the Bideshk Area, at North of Esfahan. 63 thin sections samples were studied to determine the facies. The thin sections were stained by a mixed solution of alizarin red and potassium ferrocyanide in order to distinguish between calcite and dolomite Dickson's method<sup>2</sup>. Comparative diagrams of Flugle<sup>3</sup> are also employed to calculate the percentage of the components of the rock. Having identified and determined the percentage of the skeletal, non-skeletal, cement and muddy components as well as the texture of the microscopic sections, Dunham's nomination method<sup>4</sup>, and Embry and Klován<sup>5</sup>

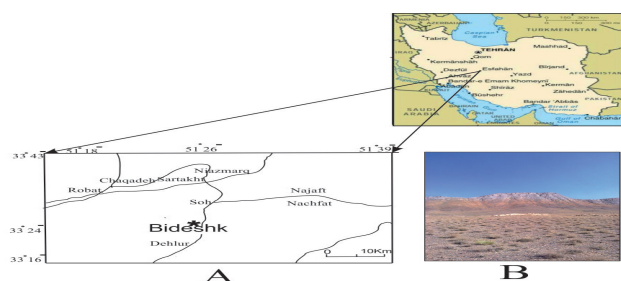


**Figure 1.** (a) Geographical location and access road. (b) Overview of Bideshk section.

and revised by Wright<sup>6</sup> was performed. Classification of carbonate microfacies is also performed based on Lasemi and Carozzi<sup>7,8</sup>. Eventually, the determined facies are compared and conformed to those of Flugel<sup>3</sup> and Wilson<sup>9</sup>. Flugel<sup>3</sup> and Walker<sup>10</sup> are also employed to present the depositional model. The facies and sedimentary environment in Bideshk area is compared with the new such as those presented in Purser<sup>11</sup> and Tucker and Wright<sup>12</sup> and old ones such as those in Read<sup>13</sup>. The sequence stratigraphy of the studied section was interpreted. We applied the concepts that were developed by many workers to determine sequence boundaries, depositional sequences (parasequences, parasequence sets) and systems tracts<sup>14-19</sup>.

## 3. Results

According to facies analysis and field observations, 4 terrigenous facies, 4 mixed facies (terrigenous and carbonate) and 10 carbonate facies are recognized as follow:

### 3.1 Continental Sub-Environment

#### 3.1.1 F1: Litharenite

This facies can be found in dark brown to red colors and compose of: quartz (50%: 0.1 mm in diameter), siliciclastic rock fragment (40%: 1.5 mm in diameter) and feldspar (5%: 2.1 mm in diameter) [Figure 2 (a) and (b)]. In some spacements of this mature facies ferroanoxide cement and dolomitization can be seen.

#### 3.1.2 F2: Feldspathic Litharenite

In this facies, limestone fragments (41%: 1.5 mm in diameter), feldspar (35%: 0.1 mm in diameter), quartz (10%: 0.1 mm in diameter) and chert (10%: 1.2 mm in diameter) easily can be seen. All the grains are sub rounded and Ferroanoxide cement and dolomite filled the pores. Sorting of the facies is nearly well [Figure 2 (c) and (d)].

#### 3.1.3 F3: Lithic Arkose

Grains of this facies include 50% feldspar, 34% siliciclastic rock fragment and 13% quartz. Average diameter of these well sorted grains is 0.2mm. Ferroanoxide cement and dolomite filled the pores [Figure 2 (e) and (f)].

#### 3.1.4 F4: Arkose

This facies can be found in dark brown and composes of feldspar (%63), quartz (%20) and siliciclastic rock

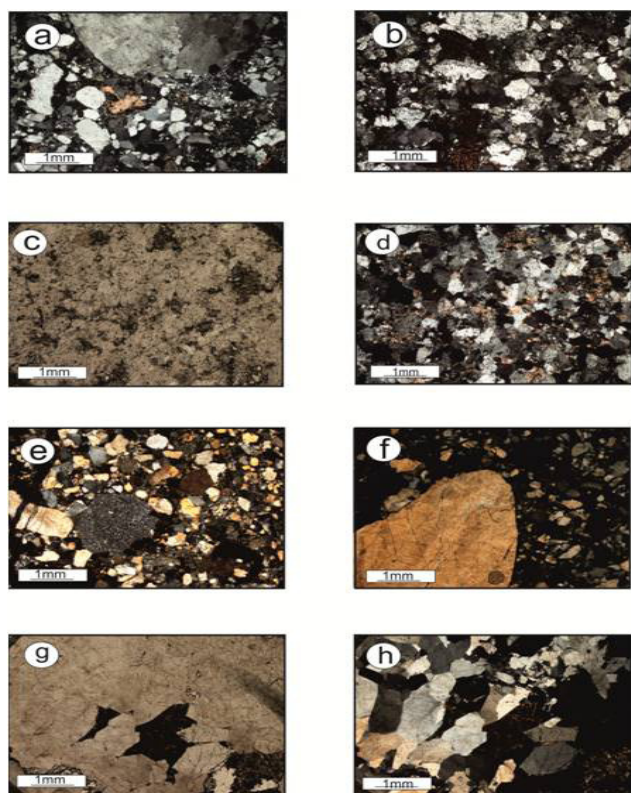


**Figure 2.** Continental environment facies. (a, b) F1: Litharenite (xpl). (c, d) F2: Feldspathic Litharenite [c (ppl) and d (xpl)]. (e, f) F3: Lithic Arkose (xpl). (g, h) F4: Arkose [g (ppl) and h (xpl)].

fragment (%7). These poorly sorted and sub rounded grains are surrounded by ferroanoxide cements ([Figure 2 (g) and (h)].

### 3.1.5 Interpretation

All of these facies have a lot of unstable grains (feldspar and rock fragment) that show they have been deposited in a subaerial conditions. Their textural properties, such as sorting and roundness support this conclusion and release that they weren't deposited in a high energy and submerged conditions<sup>20,21</sup>.

## 3.2 Tidal Flat Sub-Environment

### 3.2.1 F5: Muddy Sandstone

This facies is pale and dark brown and consists of quartz (55%: 0.1mm in diameter), lime mud (36.5%), other grains consist of echinoderm (%3), intraclast (2%), serpulid (2%), Rudist (1%) and orbitolina (0.5%) [Figure 3 (a)].

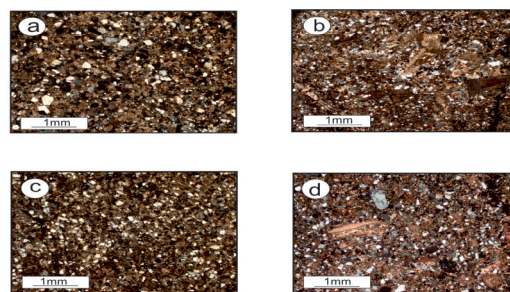


**Figure 3.** Tidal flat sub- environment facies. (a) F5: Muddy sandstone (xpl). (b) F6: Allochemic sandstone (xpl). (c) F7: sandy Limestone (xpl). (d) F8: Sandy Allochems Limestone (xpl).

### 3.2.2 F6: Allochemic Sandstone

This facies is pale brown and formed of quartz (60%), feldspar (16%: 1mm in diameter), siliciclastic rock fragment (3%: 1.5mm in diameter) and bioclast (such as Rudist 8%, Ooid 7%, Foraminifera 5%, echinoderm 1%) [Figure 3 (b)].

### 3.2.3 F7: Sandy Limestone

This facies is yellow to pale brown and composed of dolomitic cement (55%: 0.07mm in diameter) that this dolomite of kind tiny grain (20–50  $\mu\text{m}$  and yellow colors), quarts (34%: 0.08mm in diameter), feldspar (8%: 0.3mm in diameter) and siliciclastic rock fragment (3%: 0.1mm in diameter [Figure 3 (c)].

### 3.2.4 F8: Sandy Allochems Limestone

This facies is composed of Pelloid 40%, Ooid 10%, Echinoderm 3%, quartz (14%: 0.1mm in diameter), feldspar (5%: 0.7mm in diameter), chert (3% 0.5mm in diameter) with weak sorting and semicircular grains. Amount of dolomitic and limestone cement is (25%). This fine-grained dolomite (20–50 $\mu\text{m}$ ) forms the majority of the ground mass of the rock [Figure 3 (d)].

### 3.2.5 Interpretation

The fabric and the tiny size of dolomite crystals and reserved primary sedimentary texture indicate that they have been created in low temperature and near the surface of the depositional environment<sup>22</sup>. Regularly, this kind of dolomite is formed with sedimentation simultaneously or at initial stages of diagnosis in supratidal to high intertidal<sup>23</sup>.

In mixed sediment systems, transformation of carbonate sediment to siliceous-terrigenous and the entrance of sediment to the basin is in control of different factors such as climate changes, tectonic of the location, changes of water level and inside basin currents. (For example currents along the shore)<sup>24,25</sup>.

The admixture of iron oxides derived from continental zone may responsible for the formation of ferroan dolomite and make the reddish appearance of the facies<sup>26</sup>.

### 3.3 Open to Semi-Restricted Lagoon Sub-Environment

#### 3.3.1 F9: Lime Mud Mudstone

Lime mud generally comprises from 90 to 100 percent of this rock while carbonate and non-carbonate grains are rare. This rare grains consists of about %2 echinoderm (0.5mm in diameter), 1.3% Rudist (0.4mm in diameter), 1.4% Foraminifera (0.3mm in diameter), Ostracod (0.97%: 0.1mm in diameter), and some detrital contain of: orbitolina, Pelloid and quartz (less than 2% of the total grains) [Figure 4 (a) and (b)].

#### 3.3.2 F10: Orbitolina Spars Wackstone

This facies is composed of about 74% lime mud, 12.8% orbitolina foraminiferal skeleton, ranging from 1.5–1.8mm in diameter, and 4.2% ruddiest bioclasts (1–1.5mm in diameter), 2.5% Echinoderm (0.7 mm in diameter), 2.3% pelloid (0.5mm in diameter). Other grains consist of miliolid, serpulid, intraclast of the total grains. Detrital quartz (less than 5%) is also present. Silicification, slim structure and bioturbation are present in these facies which are thin -to- medium bedded [Figure 4 (c)].

#### 3.3.3 F11: Ostracod, Foraminifera Spars Wackstone

This facies is composed of about 68% lime mud and foraminifera with mean long axis with diameters of 1.3mm that comprise 13.7%, ostracod 10.2%. Echinoderm with 3.7%, serpulid and Pelloid with 0.57% is the other skeletal and non-skeletal grains in this facies. Very fine-grained quartz (less than 5%) with an average diameter of 0.1mm is also present [Figure 4 (d) and (e)].

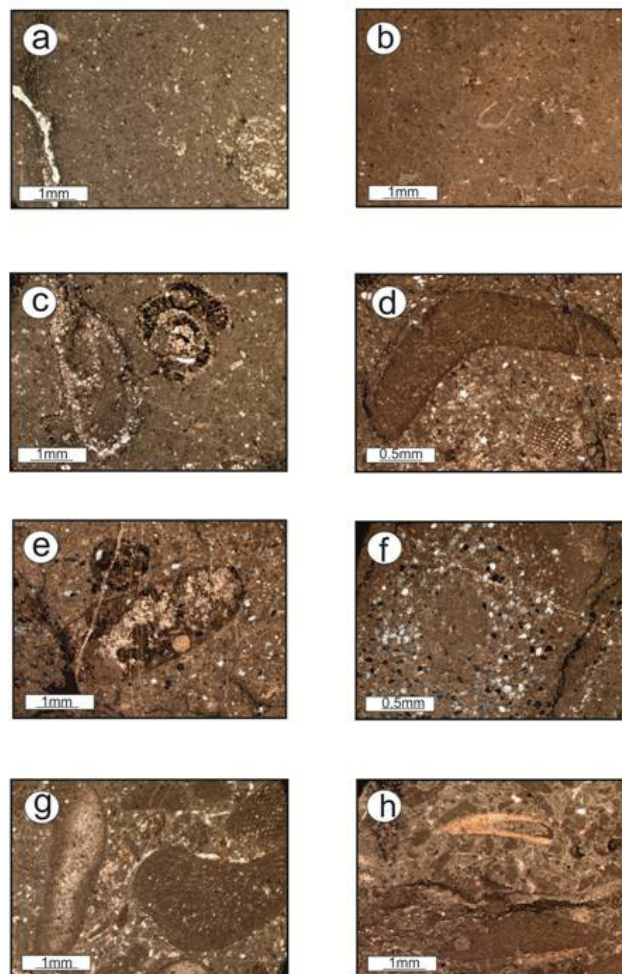


**Figure 4.** Open and semi-restricted lagoon facies. (a, b) F9: lime mud mudstone. (c) F10: orbitolina, foraminifera spars wack stone. (d, e) F11: Orbitolina spars wack stone. (f, g) F12: Rudist, Orbitolina Packstone. (h) F13: Miliolid, Pelloid pack stone (all of figures xpl).

#### 3.3.4 F12: Rudist, Orbitolina Packstone

In this facies, orbitolina (40%, 2–3mm in diameter), rudist (13%, 1–1.2mm in diameter), echinoderm (7%, 0.5mm in diameter), miliolid (7%, 0.7 mm in diameter) and other skeletal and non-skeletal grains this facies includes: intraclast, serpulid, gastropoda, pelloid, green algae, bryozoans (less than 5%) were seen. In this facies rudist with micritic rim, bioturbation and silicification were observed [Figure 4 (f) and (g)].

#### 3.3.5 F13: Miliolid, Pelloid Packstone

This facies is composed of (about 43.2%) pelloid, ranging from (0.2–0.5 mm in diameter), and (20.8%) miliolid

(0.1–0.3 mm in diameter). Other bioclasts consist of echinoderm, orbitolina, rudist, ostracod and ooid of the total grains. A few number of miliolids to pelloid was transformed and in the ground bioturbation was seen [Figure 4 (h)].

### 3.3.6 F14: Rudist, Pelloid Packstone

This facies includes: pelloid (29.3%: 0.5mm in diameter), rudist (16.6%: 1.2mm in diameter), orbitolina (7.3%: 1.5mm in diameter), echinoderm (6.6%: 0.7mm in diameter), and fragment serpulid, foraminifera, were observed. In this facies rudist with micritic rim, bioturbation and silicification were seen [Figure 5 (a)].

### 3.3.7 F15: Coral, Rudist Floatstone

This facies can be easily differentiated in the field and in the thin-sections by the large shells of rudists (%17.3: 10mm in diameter) and coral (%10: 5mm in diameter). The other skeletal and non-skeletal grains include: Orbitolina (%3.68: 1.5mm in diameter), Echinoderm (%1.84: 0.5 mm in diameter), Ostracod (%1.47: 0.9 mm in diameter), Pelloid (%0.18: 1mm in diameter), Matrix materials in this facies consist of micritized bioclasts, intraclasts, and abundant lime mud (%65) [Figure 5 (b)].

### 3.3.8 F16: Echinoderm, Orbitolina, Rudist, Rudstone

This facies of relatively complete rudist with mean long axis with diameters of 10 mm that comprise 33.7% of the total grains, Other bioclast include: Orbitolina 26.7% (3

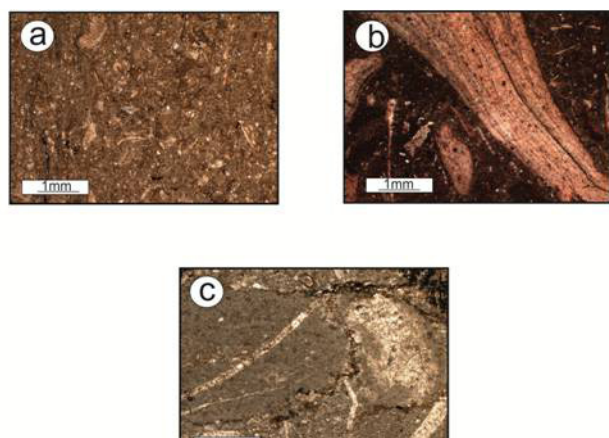


**Figure 5.** Other Open and semi-restricted lagoon facies. (a) F14: Rudist, Pelloid packstone (xpl). (b) F15: Coral, Rudist Floatstone (xpl). (c) F16: Echinoderm, Orbitolina, Rudist, Rudstone (ppl).

mm in diameter), echinoderm 17%, foraminifera 4.9% and serpulid 4% [Figure 5 (c)].

### 3.3.9 Interpretation

Common features of this Group of facies are: The presence of lime mud between the main grains and the presence of bioclastics of lagoon organisms that are able to live in restricted and semi-restricted conditions<sup>27,28</sup>. The first common feature is peace in their establishment environment and the second feature is high salt content in bottom sediments of this group. The difference between facies of this group is more fabric kind and their grain size<sup>21</sup>. Small and large algae and foraminifera have been seen in facies of euphotic zone, the zone in which water depth and nutrients are low<sup>29,30</sup>. Another distinguishing characteristic of this facies is the bioturbation that is often the result of in fauna creature's biological activity and represents sedimentation of facies in relatively quiet environment with slow water circulation and below the line of waves effect the location of creation of facies is low-depth lagoon parts in low ambient energy condition<sup>31</sup>. The location these facies is at deeper lagoon parts with low ambient energy conditions. Entity bentic foraminifera (for example miliolid) and also conical orbitolina indicative of low-energy environments and extensive pelloids also suggest that these low-energy environments were both shallow and restricted<sup>27,28</sup>.

## 3.4 Shoals Sub-Environment

### 3.4.1 F17: Miliolid Grainstone

This facies contains miliolid (31.4%: 0.5 mm in diameter), green algae (8.5%: 0.7 mm in diameter), orbitolina (6.4%: 2.2mm in diameter), ooid (6.3%: 0.5 mm in diameter), rudist (5.7%: 1.3mm in diameter), echinoderm (5%: 1.1 mm in diameter), bivalve (3.5%: 0.7 mm in diameter), aggregate grains (3.2%: 1.1 mm in diameter) and between grains sparry cement is present. In this facies sorting and circular grains are present [Figure 6 (a) and (b)].

### 3.4.2 F18: Orbitolina, Ooid Grainstone

This facies is characterized by well-sorted radial and superficial oolite grains (0.25–0.5mm) that account for about %28.2 of the rock. Their nuclei consist of green algae, miliolid, bivalve, rudist, echinoderm and aggregate grains. Skeletal components include bioclasts of orbitolina (16.2%: 1.5mm in diameter), miliolid (5.5%: 0.5 mm in

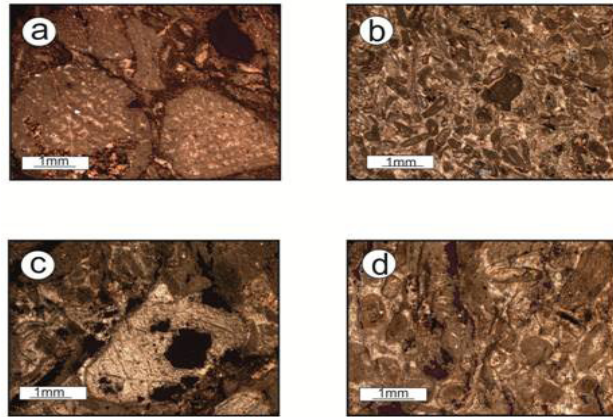


**Figure 6.** Shoal and bar facies. **(a, b)** F17: Miliolid Grainstone (xpl). **(c, d)** F18: orbitolina, Ooid Grainstone (xpl).

diameter), rudist (4.2%: 1–1.2mm in diameter), intraclast (2.9%: 1mm in diameter), echinoderm (%2.6: 1–1.5mm in diameter). Minor particles are green algae, bivalve, aggregate grains gastropoda and between grains sparry cement are present. In this facies sorting and circular grains are present [Figure 6 (c) and (d)].

### 3.4.3 Interpretation

The lack of lime mud sediments in this sub-environment shows high energy rate<sup>27,28</sup>. In other words, these facies are created above wave's effective line. Facies related to ooid, bioclastic and shoal bars are created at sub-environment of platform margin. Skelet on particles such as echinoderms are seen in slop area and can cause the creation of washed sandy sediments of shoal or bar<sup>21,27,28</sup>. Sparite cement, ooids, well sorting and lack of lime mud in facies indicates an environment with high energy. Waves and flows have affected transportation of carbonate grains. Skeletal and fragments of these sands are usually originated of open sea<sup>21</sup>. Large size of particles in these facies and approximate sorting of these particles are of other indicative factors of high energy in these facies.

## 4. Sedimentary Model of Bideshk Area

According to the field and thin section studies, vertical relationships of facies and comparing bideshk area facies with different sedimentary facies models in this model, four sedimentary sub-environment are distinguished that include: continental, tidal flat, lagoon and bar. Sandstone

sedimentations relate to the continental environment. These facies are created at a mixed carbonate ramp of low slope of homoclinal kind<sup>32–36</sup>. In this model, continental sub-environment was location of creation of sandstone sediments and that shows the weak weather of that environment. In Intratidal sub-environment, phenomena such as the fabric and the tiny size of dolomite crystals and reserved primary sedimentary texture indicate that they have been created in low temperature and near the surface of the depositional environment. This kind of dolomite is formed with sedimentation simultaneously or at initial stages of diagenesis in supratidal to high intertidal.

Lagoon sub-environment sediments are separated from shoal and tidal flat<sup>23</sup>. The presence of lime mud between the main grains and the presence of bioclastics of lagoon organisms that are able to live in restricted and semi-restricted conditions<sup>27,28</sup>.

Shoal sub-environment was in this model highest energy portion of the environment was location to of creation of craying sediments (Figure 7).

## 5. Sequence Stratigraphy

Sequence stratigraphy is a method of classification and interpretation of sedimentary rocks and fossils in the changing environments<sup>35–39</sup> Changes in climate and relative sea level can be detected through careful analysis of sequence stratigraphy<sup>27</sup>. Sequence boundary coincides with a drop in relative sea level and is mostly widespread during the most drop of this level. These boundaries are divided into two kinds: Sequences boundary of the first type SB1 and sequence boundary second type SB2<sup>27</sup>.

The general vertical facies succession through the Bideshk area and the stacking patterns and upward changes in the parasequences permit the identification of sequences and their component systems tracts within the succession.

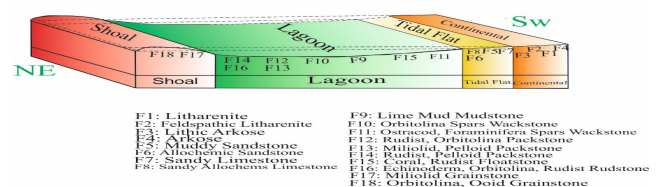


**Figure 7.** Sedimentary environment model of Bideshk area.

Based on the sequence surfaces (SB, TS, MFS) and according to Fishers method<sup>19</sup> and Martin-Chivelets method<sup>18</sup> three third-order depositional sequences of the study area are recognized as follow (Figure 8).

### 5.1 Sequence 1

Lower boundary in the first sequence is unconformity first type Boundary (SB1) (with Jurassic deposits) and consists of Transgressive Systems Tract (TST). They have an aggradational stacking pattern. The only portion of the sequence is Transgressive Systems Tract (TST) that is composed of brown, thick bedded sandstone facies (arkose, litharenite, lithic Arkose and feldspathic litharenite) so this sequence composed of continental sediments.

### 5.2 Sequence 2

The thickness of sequence 2 is nearly 120m and started with first type (SB1) sequence boundary. This sequence is a complete sequence and composes of Lowstand Systems Tract (LST), Transgressive Systems Tract (TST) and Highstand Systems Tract (HST). LST is composed of light brown, medium bedded mixed carbonate and terrigenous facies. So this portion of sequence was deposited in the intertidal. TST includes a set of lagoon (retrogradational) parasequences. These parasequences include of: bioclast grainstone, ooid Grainstone. HST also is composed of bar and lagoon aggradational facies.

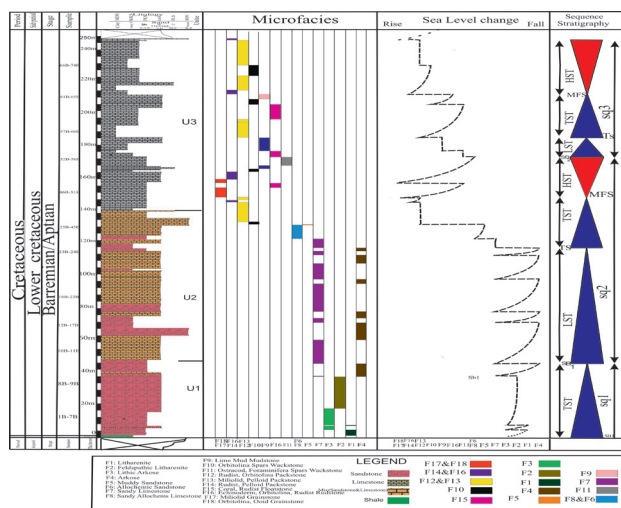


**Figure 8.** Microscopic facies column and sequence stratigraphy of Bideshk area.

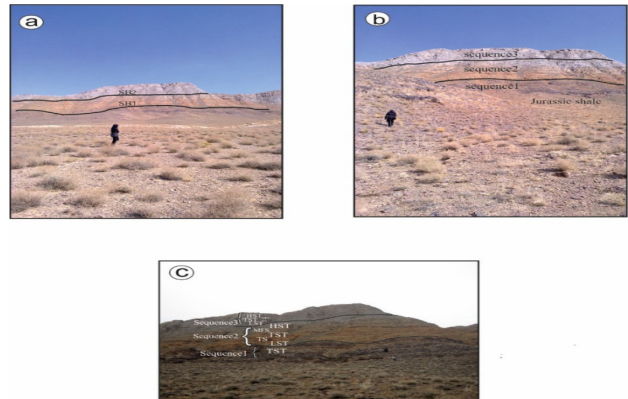


**Figure 9.** (a) Overview of Bideshk section with sequence boundary of SB1 and SB2. (b) View of 3 sequence of Bideshk section. (c) Overview of Bideshk section with separated sequences of considered.

### 5.3 Sequence 3

This sequence commences with second type Sequence Boundary (SB2). The thickness of this sequence is nearly 85m. This sequence is a complete sequence too and includes of LST, TST and HST and entirely composed of lagoon facies. This sequence facies are the deepest facies of the succession (Figure 8, 9).

## 6. Conclusion

The Bideshk area represents sedimentation on a homoclinal carbonate ramp. 18 facies were recognized within this carbonate platform section. They are grouped into four depositional environments representing continental, tidal flat, Open to semi-restricted Lagoon and shoal. Three third-order depositional sequences are identified from shallowing and deepening trends of depositional facies and changes in the cycle stacking pattern. Lower boundary in the first sequence is unconformity first type boundary (SB1) (with Jurassic deposits) and consists of Transgressive Systems Tract (TST). Sequence number 2 consists of Lowstand Systems Tract (LST), Transgressive Systems Tract (TST) and Highstand Systems Tract (HST) and started with first type (SB1) Sequence Boundary. Sequence 3 also consists of LST, TST and HST and started with second type (SB2) Sequence Boundary.

## 7. References

1. Khosrow Tehrani KH. Geology of Iran Mesozoic and Cenozoic. Tehran: Keledar; 2006. p. 456.

2. Dickson JAD. Stains for carbonate minerals. In: Middleton GV, editor. *Encyclopedia of Sediments and Sedimentary Rocks*. Dordrecht: Kluwer Academic Publishers; 2003. p. 683–4.
3. Flügel E. *Microfacies of Carbonate Rocks, Analysis, Interpretation and Application*. Berlin, Heidelberg: Springer Verlag; 2010. p. 976.
4. Dunham RJ. Classification of carbonate rocks according to depositional textures. In: Ham WE, editor. *Classification of carbonate rocks, a symposium*. AAPG Me; 1962. p. 108–21.
5. Embry AF, Klovan JE. A Late Devonian reef tract on north-eastern Banks Island, Northwest Territories Bull. Canadian Petrol Geol. 1971; 19:730–81.
6. Wright VP. A revised Classification of limestone. *Sedimentary Geology*. 1992; 76(3):177–85.
7. Lasemi Y, Carozzi AV. Carbonate microfacies and depositional environments of the kinkaid formation (Upper Mississippian) of the Illinois Basin. V.S.A. 8th congress Geol Argention, Sanluis, Actas 2; 1981. p. 357–84.
8. Carozzi AV. Carbonate rocks depositional model. New Jersey: Prentice Hall; 1989. p. 604.
9. Wilson JL. Carbonate facies in geological history. Berlin: Springer-verlag; 1975. p. 471.
10. Walker R, James NP. Facies, facies models and modern stratigraphic concepts. *Facies Models: Response to Sea-level Change*. Geological Association of Canada; 1992. p. 1–14.
11. Purser BH. *The Persian Gulf*. Springer-Verlag publication; 1973. p. 471.
12. Tucker ME, Wright VP. *Carbonate Sedimentology*. Blackwell Scientific Publication; 1990. p. 496.
13. Read JF. Carbonate platform facies models. *Bull Am Assoc Petrol Geol* 69; 1985. p. 1–21.
14. Wagoner VJC, Posamentier HW, Mitchum RM, Vail PR, Sarg JF, Loutit TS, et al. An overview of sequence stratigraphy and key definitions in sea level changes. *SEPM Spe Publ*. 1988; 42:39–45.
15. Wagoner VJC, Mitchum RM, Champion KM, Rahmanian VD. Siliciclastic sequence stratigraphy for high resolution correlation of time and facies. *AAPG Meth Explora seri*; 1990. p. 7–55.
16. Loucks RG, Sarg JF. Carbonate sequence stratigraphy. *AAPG Mem*. 1993; 57:545.
17. Emery D, Myers K. *Sequence stratigraphy*. Oxford: Blackwell; 1996. p. 297.
18. Martin-Chivelet J. Quantitative analysis of accommodation patterns in carbonate platforms: An example from the mid-Cretaceous of SE Spain. *Journal of Palaeogeography, Palaeoclimatology, Palaeoecology*. 2003; 200(1–4):83–105.
19. Fischer AG. The Lofer cyclotherms of the alpine triassic kan-sas. *Journal of Geology Survey*. 1964; 169(1):107–49.
20. Nebelsick JH, Rasser D, Lwmp J. Tracking paleoenvironmental changes in corall algal-dominated carbonates of the Lower Oligocene Calcareniti di castelgomberto formation (Monto Berici, Italy), *Facies*. 2013; 59:133–48. Available from: <http://dx.doi.org/10.1007/s10347-012-0349-6>
21. Yang W, Feng Q, Liu Y, Tabor N, Miggins D, Crowley JL, et al. Depositional environment and cyclo-and chronostratigraphy of uppermost Carboniferous-Lower Triassic fluvial-lacustrine deposits, southern Bogda Mountains, NW China-A terrestrial paleoclimatic record of mid-latitude NE. *Global and Planetary Change*. 2010; 73(1–2):15–113.
22. Gregg JM, Shelton KL. Dolomitization and neomorphism in the back reef facies of the Bonnetterre and Davies formations (Cambrian), southeastern Missouri. *Journal of sedimentary petrology*. 1990; 60(4):549–62.
23. Adabi MH. Petrography and geochemical criteria for recognition of unaltered cold water and diagenetically altered Neoproterozoic dolomite, western Tasmania. *16th Australian Geol con v, Australia(Abst)*; 2002. p. 350.
24. Budd DA, Harris PM. Carbonate siliciclastic mixtures. *SEPM Reprint series*. 1990; 26:185–204.
25. Musavizadeh MA, Mahboubi A, Moussavi-Harami R, Najafi M. Identification of Types and Formation Mechanisms of Dolomite Mineral in the limestone of Tirgan Formation in the West of Kopet-Dagh. *Proceedings of the fifteenth meeting of the Association of crystallography and mineralogy Ferdowsi university of Mashhad, Iran 2008*. p. 347–52.
26. Zonneveld JB, Gingras MK, Pemberton SG. Trace fossil assemblages in a Middle Triassic mixed siliciclastic-carbonate marginal marine depositional system, British Columbia. *Palaeogeogrpalaeoclimatol palaeoecol*. 2001; 166(3–4):249–76.
27. Mahboubi A, Moussavi-Harami R, Mansouri-Daneshvar P, Najafi M, Brenner R. Upper Maastrichtian depositional environments and sea-level history of the Kopeh-Dagh. *Intracontinental Basin, Kalat Formation, NE Iran: Springer-Verlag*; 2006. p. 237–48.
28. Amirshahkarami M, Vaziri Moghaddam H, Taheri A. Sedimentary facies and sequence stratigraphy of the Asmari Formation at Chaman-Bolbol, Zagros Basin, Iran. *Journal of Asian Earth Sciences*. 2007; 29(5–6):947–59.
29. Bromley RG. *Trace fossils: Biology and Taphonomy*. London: Unwin Hyman LTD; 1990.
30. Lasemi Y. Depositional environments of the Ordovician rocks of Iran (syn-rift sequences) and formation of the Paleotethys passive margin. *17th Annual Meeting of the Geol Survey of Iran*; 1999. p. 160.
31. Flügel E. *Microfacies of Carbonate Rocks, Analysis, Interpretation and Application*. New York: Springer-Verlag; 2004. p. 996.

32. Basso D, Nalin R, Nelson CS. Shallow-water Sporrolithon rhodolith from North Island (New Zealand). *Palaios*. 2009; 24(2):92–103.
33. Desjardins PR, Buatois LA, Limarino CO, Cisterna GA. Latest Carboniferous-earliest Permian transgressive deposits in the paganzo Basin of western Argentina: Lithofacies and sequence stratigraphy of a coastal-plain to bay succession. *JS Am Earth Sci*. 2009; 28(1):40–53.
34. Sloss LL. Sequence in cratonic interior of North America. *Geological Society of America Bulletin*. 1963; 74:93–114.
35. Shahraki J, Harami MR, Mahboubi A, Jahani D. Facies Analysis, Depositional Environment and Cyclostratigraphy of the Lower Permian deposits Chili Formation in the Kalmard Block, East Central Iran (Godar-e-Gachal section). *Indian Journal of Science and Technology*. 2014; 7(10):1588–602.
36. Karimi H, Ghadimvand KN, Kangazian A. Sedimentary environment and Sequence stratigraphy of the Kangan formation in Kish gas field (Kish Well A1 Subsurface Section). *Indian Journal of Science and Technology*. 2015; 8(7):655–63.
37. Shinn A. Modern carbonate tidal flat: Their diagnostic features. *Quart J Colorado school of Mines*. 1986; 81(1):7–35.
38. Mahboubi A, Moussavi-Harami R, Lasemi Y. Sequence stratigraphy and sea level history of the upper Iran, American association of petroleum Geologists. *AAPG BULLETIN*. 2001; 85(5):839–59.
39. Odedede O, Adaikpoh EO. Sequence stratigraphic analysis of the Gombe Sandstone and lower Kerri–Kerri Formation exposed around Fika-Potiskum, Upper Benue Trough, Nigeria: A consideration for petroleum reservoir indicators. *Indian Journal of Science and Technology*. 2011; 4(5):462–98.